Simulation of flashover discharge on solar array by using plasma impedance model

Anna Kawano, Kazuhiro Toyoda, and Mengu Cho

Kyushu Institute of Technology, Department of Electrical Engineering, Kitakyushu, Fukuoka, 804-8550, Japan

Electrostatic discharges occur on solar arrays due to their interaction with space environment. Due to the complexity of space environment, electrostatic discharges should be investigated through ground based testing considering many factors. Currently, it is believed that flashovers propagate concentrically from the point of discharge. The plasma propagating from the electric discharge initiation point presents a certain resistance and inductance value that have an impact on the flashover current waveform. The purpose of this study is to model the plasma impedance for which the experimental sample used is the same model as the simulation model. From the measurements result of the discharge current and the surface potential, the plasma resistance was calculated. The calculated plasma resistance showed the same characteristics as the simulation model results.

Flashover current waveform was simulated by using resistance. However, the simulated waveform did not match the measured waveform. Therefore, the plasma inductance characteristic was taken into account as a simulation parameter. Peak current, charge, and current cut-off time simulation parameters were approximated using the measured waveform results.

Key Words: Solar Array, Flashover, Plasma

Nomenclature

V	:	voltage
I	:	neutralization current
i	:	flashover current
Q	:	charge
C	:	capacitor
R	:	plasma resistance
L	:	inductance
r	:	distance from center of the coupon
ρ	:	charge density of polyimide tape

Subscripts

0	:	differential voltage
$Before$	:	before discharge
$After$	:	after discharge
$bias$	:	biased voltage
k	:	k th electrode

1. Introduction

Charging and discharging of spacecraft solar cells arrays was reported to occur through their interaction with the space environment. When an electrostatic discharge occurs, it may affect a spacecraft by decreasing it power generation capability or even stop the spacecraft operations. Therefore, there is a need for investigating through ground based testing the charging and discharging phenomenon of solar cells.

According to previous studies, it is believed that flashover is propagated concentrically from the electrostatic discharge initiation point.[1)-5)] However, the size of ground test devices is limited and it is difficult to perform a ground test of large solar arrays. Therefore, the discharge current should be simulated. In previous studies, it was simulated using the velocity at which discharge light propagates.[6)] However, the discharge current waveform was not yet accurately simulated. In this experiment, the discharge current and the surface potential were measured. Moreover, when the discharge propagated, the resulting plasma resistance was analyzed. The present paper reports the measurements, analysis, and the simulation results of the flashovers current.

2. Charge/discharge test

2.1. Discharge currents

The coverglasses are attached to solar cells surface. When high-energy particles collide with the satellite, the satellite becomes negatively charged relatively to the surrounding environment. Upon collisions repetition, cover glass becomes positively charged relatively to the spacecraft due to a difference in secondary electron emission coefficient between insulating and conducting materials. This condition is called inverted potential gradient. When the electric potential exceeds a threshold, a discharge occurs. At the time of the discharge, electric charges stored in the cover glass are neutralized to propagate extensively. Flowing current at that time is called neutralization current. Moreover, the resulting energy that exists between the spacecraft and space is flowing to the discharge initiation point. This is called a blow-off current. There is also current flowing through the row of the solar cells, namely the flashover current. Figure 1 shows the currents flow when a discharge occurs.

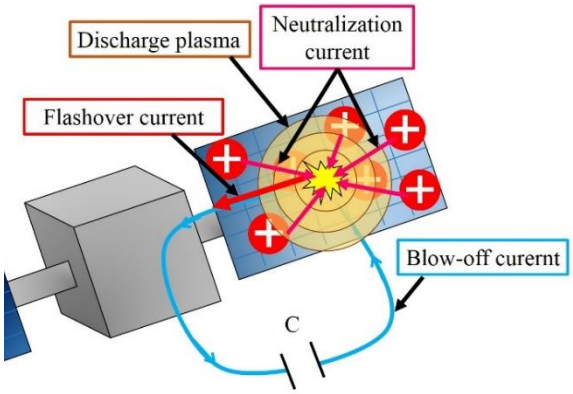

Fig. 1. Schematic of the discharge currents path

2.2. Test coupon

Figure 2 shows a test coupon (ring coupon) for charge/discharge experiment. This is a copper electrode that was cut in a ring shape and they are 11 sheets arranged concentrically. Polyimide tape was attached on the ring coupon. With this configuration, the copper electrodes simulate a solar cell and the polyimide tape simulates the cover glass. Only disks in the center of the electrode were exposed to electrons bombardment and a discharge was induced in this part as a result. The ring coupon allows the acquisition of the current waveforms, which propagate concentrically from the discharge initiation point.

The ring coupon was biased using a cable connected to each electrode and when a discharge occurred, the different currents were measured using a separated probe connected to each electrode.

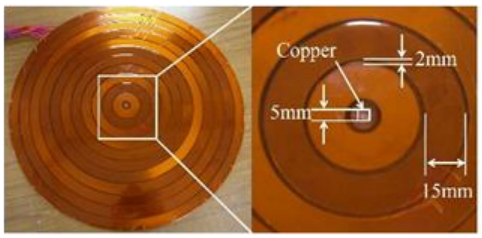

Fig. 2. Test coupon (ring coupon)

2.2. Experimental circuit

Figure 3 shows the experimental circuit. In order to simulate the inverted potential gradient, the ring coupon was biased negatively by V_{bias}. Ct simulates capacitance of satellite body.

The discharge current was measured by current probes from an external circuit. The flashover current is measured by Cp1. The neutralization current is measured by probes Cp2 to Cp12. The blow-off current is measured by probe Cp13.

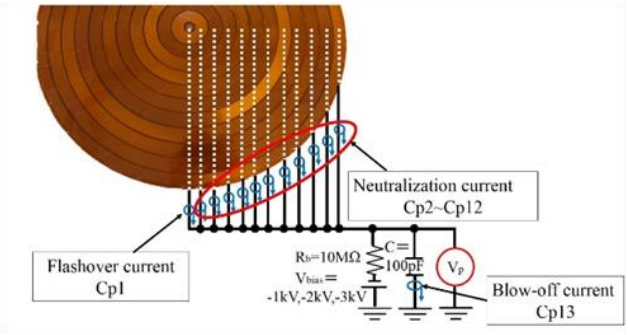

Fig. 3. Experimental circuit

2.3. Vacuum chamber

Figure 4 shows the vacuum chamber used in this study. This is cylindrical chamber with a diameter of 1.0m and depth of 1.2 m. To simulate PEO environment, the ultimate pressure was about 6×10^{-5}Pa and an electron gun as well as a plasma source were installed to simulate the high-energy particles.

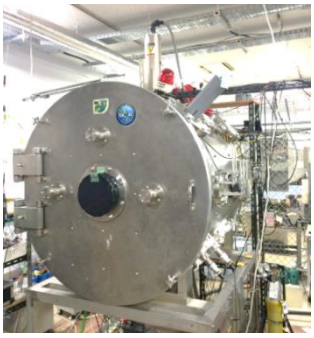

Fig. 4. Vacuum chamber

2.4. Experimental system

Figure 5 shows the experimental system. The ring coupon was placed in the vacuum chamber and the circuit was connected to the outside of the chamber.

In previous experiments, the electron beam was used to charge the ring coupon. However, with this method it is difficult to uniformly charge the ring coupon. In this experiment, an ultraviolet light (ozone producing lamp) was used to charge the ring coupons by photoelectric effect. The discharge was induced by irradiating a YAG laser toward the center of the ring coupon through a mirror from outside of the chamber.

When a discharge occurred, the discharge waveform was measured by an oscilloscope with setting a rising trigger on the bias voltage. The surface potential was measured before and after discharge using a non-contact measurement probe, namely Trek. Figure 6 shows the setting inside the chamber.

3. Analysis method

3.1. Calculation of plasma resistance

The plasma resistance was calculated from the measurement results. The neutralization current flows toward each electrode through the plasma when a discharge occurs. To determine the plasma resistance from the neutralization current, the charge Q, is calculated from the

neutralization current flowing through the plasma (Eq. 1).

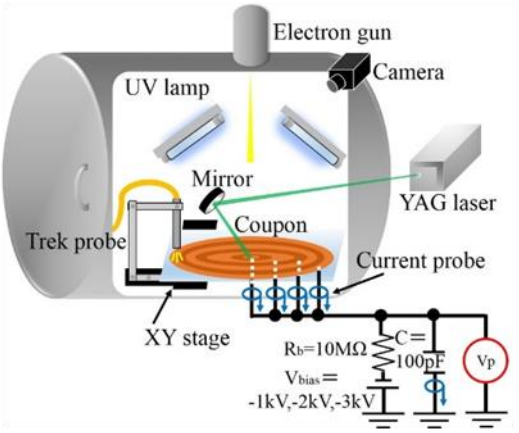

Fig. 5. Experimental system

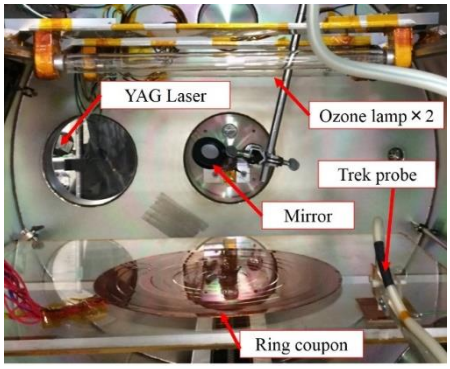

Fig 6. Settings inside the chamber

$$Q(t) = \int I(t)dt[F \bullet V] \qquad \text{(Eq. 1)}$$

Then, the polyimide tape capacitance C, from the potential difference between the voltages before and after discharge is calculated (Eq. 2).

$$C = Q / V[F] \qquad \text{(Eq. 2)}$$

From Q and C, the time variation of the charging voltage after discharge is calculated (Eq. 3).

$$V(t) = V_0 - Q(t) / C\ [V] \qquad \text{(Eq. 3)}$$

The resistance R, of the discharge plasma can then be calculated from the previously calculated neutralization current I, and voltage V (Eq. 4).

$$R(t) = V(t) / I(t)[\Omega] \qquad \text{(Eq. 4)}$$

The above calculation was applied for each electrode.

3.2. Flashover simulation[3)]

Figure 7 shows the model for the simulation of the discharge current. Discharge path of the ring coupon was divided into small sections in this simulation model. It is assumed that a resistor, inductor, and capacitor exist for each small section.

Using this model, the current flowing in each micro time was calculated. In the ring coupon, the differential potential is considered uniform. Moreover, all capacitances C_n, are considered to have been charged by voltage V.

Table 1 shows the parameters for each element. The model of the plasma resistance was considered as shown in Fig. 8. Equation 5 shows the characteristic of the plasma resistance.

Table 1. Simulation parameter

$R_k(t)$	Resistance of the k-th small area at time t [Ω]
C_k	Capacitance of the k-th small area [F]
L_k	Inductance of the k-th small area [H]
L_{line}	Inductance of line [H]
$i_k(t)$	Current of the k-th small area at time t [A]
$V_k(t)$	Potential of the k-th small area at time [V]
ρ	Charge density of the surface insulating material (Kapton : ρ=505nF/m^2) [F/m^2]
dr	Small radius [m]
dt	Small time [s]

$$R = a/\ (I - b) + \qquad \text{(Eq. 5)}$$

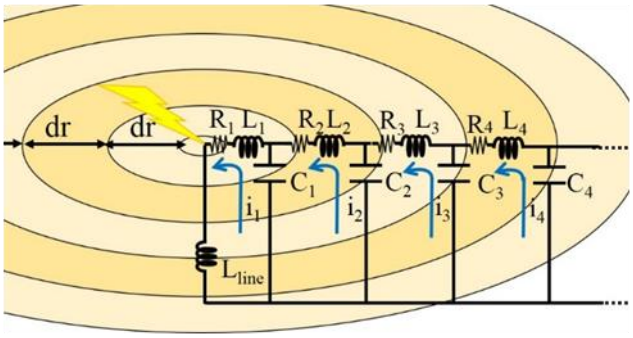

Fig. 7. Simulation model

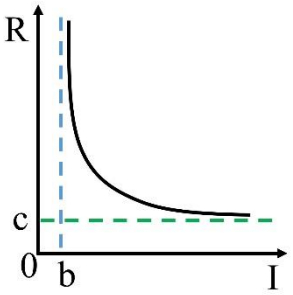

Fig. 8. Plasma resistance model

The simulated flashover current is represented from Eq. 6 to Eq. 10. The resistance, R, is a function of the total current flowing through R (Eq. 6). R is divided by k for taking into account that the current increases with the increase of the radius r. The capacitance, C, is a function of r (Eq. 7). The inductance, L, is divided by k to take into account that it decreases with the increase of r (Eq. 8). The voltage, V_k (t), was calculated from the charging of the capacitor at V = Q / C (Eq. 9). Q decreases as the current flows. Therefore, it is a function of the charge flowing from C at time t. The

flashover current, i_k, was calculated from the difference between the current flowing through V/R and L (Eq. 10). Finally, the differential voltage after the discharge and the discharge current of each differential time dt was calculated.

$$R(t) = \frac{1}{k}\sqrt{\left(\frac{a}{\sum_{k'=k}^{n} i_{k'}(t) - b} + c\right)^2}\ [\Omega] \quad \text{(Eq. 6)}$$

$$C_k = 2\pi dr \cdot kdr \cdot \rho [F] \quad \text{(Eq. 7)}$$

$$L_k = \frac{L_0}{k}[H] \quad \text{(Eq. 8)}$$

$$V_k(t) = \frac{C_k V_0 - \sum_{t'=0}^{t} i_k(t')}{C_k}[V] \quad \text{(Eq. 9)}$$

$$i_k(t) = \frac{V_k}{\sum_{k'=0}^{k} R_{k'}} - \frac{(\sum_{k'=0}^{k} L_k + L_{line}) \times \frac{\frac{V_k(t)}{\sum_{k'=0}^{k} R_{k'}} - i_k(t-dt)}{dt}}{\sum_{k'=0}^{k} R_{k'}}[V] \quad \text{(Eq. 10)}$$

4. Measurement results

4.1. Discharge current

Figure 9 shows the discharge current waveform for V_{bias}=-1kV. The neutralization current begins to flow in all of the electrodes. At the same time the discharge current flows. The discharge plasma is considered to be propagating throughout the ring coupon. The plasma resistance was calculated using the neutralization current. The flashover current waveform at each bias voltage was compared as shown in Fig. 10. The peak value of the current is increased when the bias voltage increases.

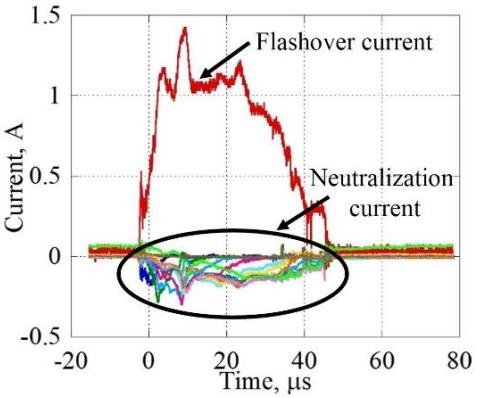

Fig. 9. Discharge waveform for V_{bias}=-1kV

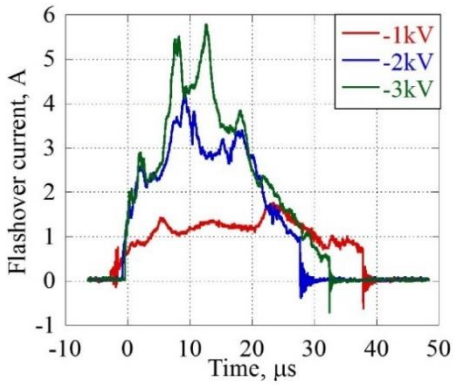

Fig. 10. Comparison of the flashover waveforms

4.2. Surface potential

Figure 11 shows the surface potential before the discharge for each bias voltage. For V_{bias} = -1kV, -2kV, and -3kV, the ring coupon was charged to about 840V, 1450V, and 1850V, respectively. These value is called a potential difference V_0.

Figure 12 shows the surface potential after the discharge for each potential difference. The surface potential concentrically decreased. It indicates that the discharge plasma propagated concentrically and neutralized the charge.

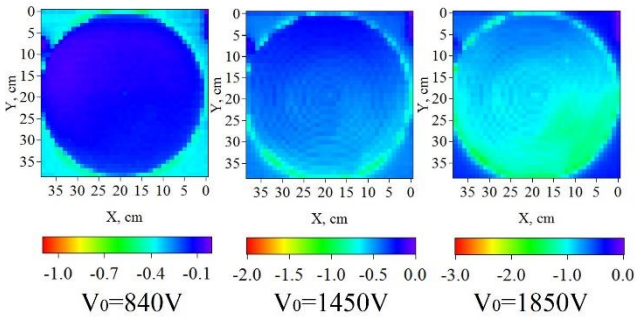

Fig. 11. Surface potential before discharge for each V_0

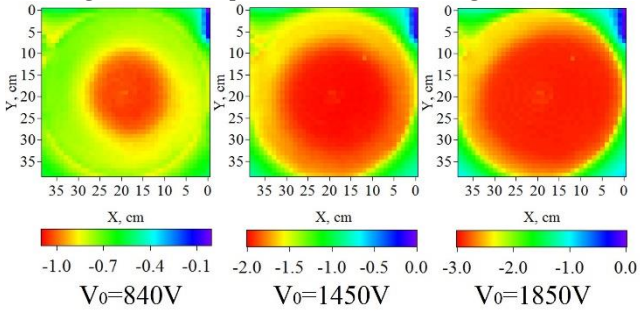

Fig. 12. Surface potential after discharge for each V_0

As shown in Fig. 13, 1D data of the surface potential before and after the discharge was extracted. From Eq. 11, the ratio of charge responsible for neutralization (neutralization ratio) was calculated.

Figure 14 shows the neutralization ratio for each potential difference. According to this figure, it can be concluded that the neutralization charge also increases when the potential difference increases.

$$\frac{V_{Before} - V_{After}}{V_{Before}} \times 100\ [\%] \qquad \text{(Eq. 11)}$$

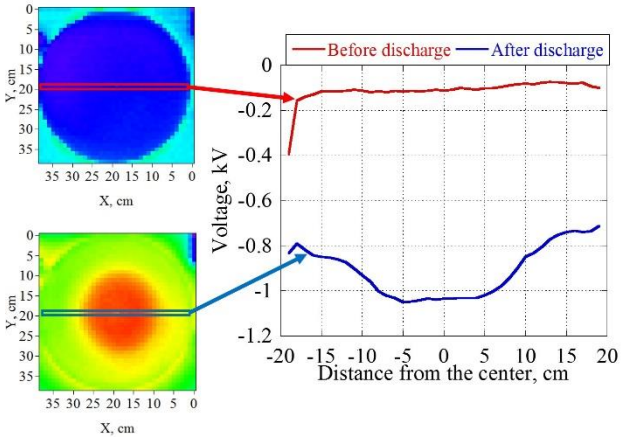

Fig. 13. 1D data extraction of the surface potential before and after discharge

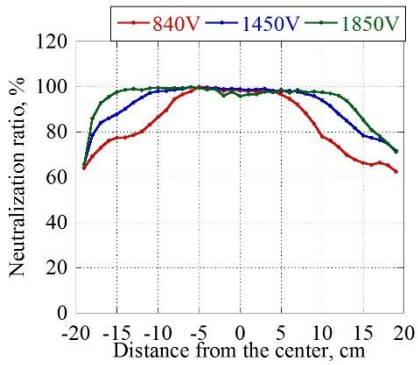

Fig. 14. Neutralization ratio for each V_0

5. Simulation

5.1. Calculation of plasma resistance

Characteristics of the plasma resistance to be used in the simulation were calculated using Eqs. 12 and 13. From Eq. 12, the total neutralization current flowing through the k-th electrode was calculated. From Eq. 13, the plasma resistance on the k-th electrode was calculated.

Figure 15 shows the characteristics of the plasma resistance. X-axis is the neutralization current flowing through each electrode, Y-axis is the plasma resistance on the electrodes. Regression curve in the Fig. 15 was consistent with the characteristics of the plasma resistance to be used in the simulation.

As shown in Fig. 15, the simulation parameters were calculated by taking the average of the regression curve (Table 2.).

$$I_k = \sum_{k'=k}^{n} I_{k'}(t) \qquad \text{(Eq. 12)}$$

$$R_k' = R_k - R_{k-1} \qquad \text{(Eq. 13)}$$

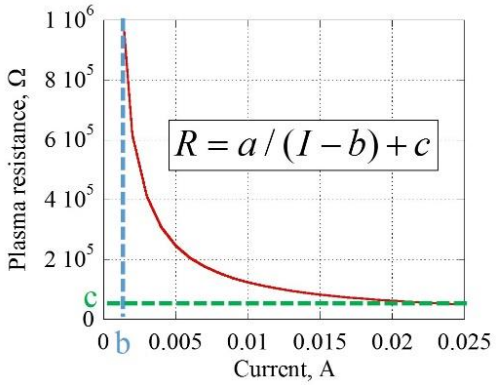

Fig. 15. Calculated plasma resistance

Table 2. Simulation parameters

P		505nF/m^2
Dr		0.005m
Dt		1ns
N		39
A		1164
B		5mA
C		1000Ω
V_0 [V]	V_{bias} = -1kV	840
	V_{bias} = -2kV	1450
	V_{bias} = -3kV	1850

5.1 Simulation results

5.1.1 Plasma resistance characteristics

Using the values in Table 2, the surface potential and the flashover currents were simulated. Figures 16 to 18 show the results of comparing the calculated values with the experimental values of the flashover current. Table 3 shows a comparison of the charge for each potential difference. For the flashover current, the calculated and measured values are different at the peak value and it was not possible to obtain a waveform along the experimental values. However, the calculated charge values were nearly equal to the average of the experimental values.

Figure19 shows a comparison of the flashover current for *b* = 0 or 0.005. It was possible to show the characteristics of the current cut-off, like the experimental values of flashover current, by using the value of *b* as a characteristic of plasma resistance.

Figure 20 shows the result of neutralization simulation for each potential difference. The area of neutralization increased when the potential difference increased. It shows similar characteristics with the experimental values.

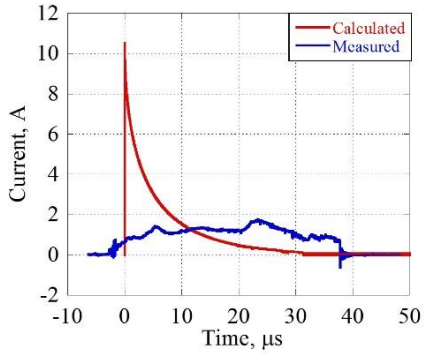

Fig. 16. Comparison of the flashover currents for V_0 = 840V

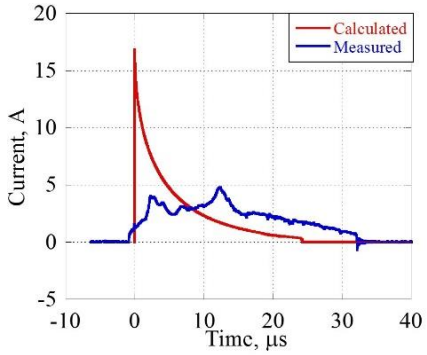

Fig. 17. Comparison of the flashover currents for V_0 = 1450V

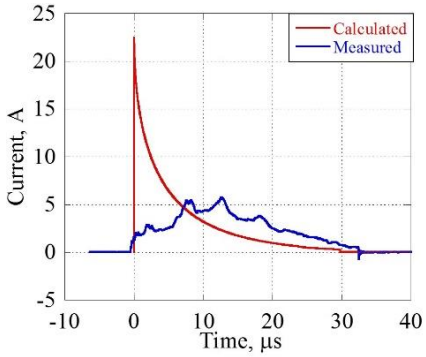

Fig. 18. Comparison of the flashover currents for V_0 = 1850V

Table 3. Comparison of calculated and measured charge Q

V_0 [V]	Q [μC]	
	Calculated	Measured (Average)
840	49.1	50.1
1450	72.4	76.3
1850	100.2	102.4

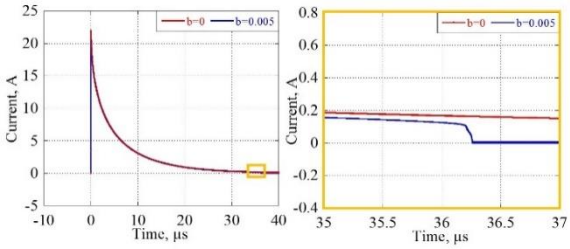

Fig. 19. Comparison of the flashover current for different b. (Left side: overall figure of flash over current. Right side: enlarged figure of the current cut-off part)

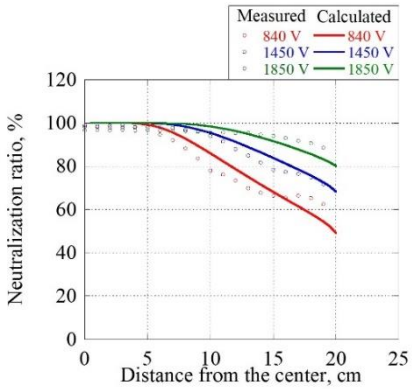

Fig. 20. Comparison of the neutralization ratio for each V_0

5.1.1 Plasma resistance and inductance characteristics

Flashover current and surface potential were simulated taking into account the plasma resistance and inductance. The inductance was adjusted to be approximately equal to the peak value and the charge of the experimental values. For the other parameters, values presented in Table 2 were used.

The inductance values used in the simulation are shown in Table 4. The calculated and experimental values of the charge for each differential voltage are also shown in Table 4.

For differential voltages V_0 = 1450V and 1850V, it was possible to approximate the charge of experimental values by adjusting L. However, in the case of the differential voltage V_0 = 840V, it was not possible to approach the experimental values.

Table 4. Comparison of calculated and measured charge Q taking into account the inductance L

V_0 [V]	L_0 [μH]	L_1 [μH]	Q [μC]	
			Calculated	Measured (Average)
840	1.3	0.005	38.4	50.1
1450			76.4	76.3
1850			101.7	102.4

Figures 21 to 23 show the comparison results of the experimental and calculated values of flashover current. As compared to the calculations taking into account only the

plasma resistance (Figs.16 to 18), when the inductance is also taken into account, it was possible to approximate the peak value and the current cut-off time of the experimental value for the differential voltages V_0 = 1450V and V_0 = 1850V. Figure 24 shows the neutralization ratio and it exhibits the same characteristics presented in Fig. 20.

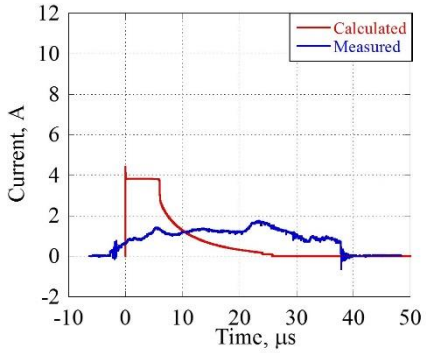

Fig. 21. Comparison of the flashover currents for V_0 = 840V

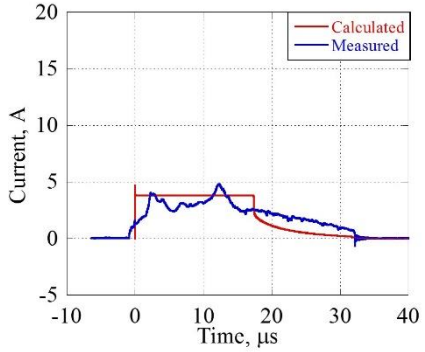

Fig. 22. Comparison of the flashover currents for V_0 = 1450V

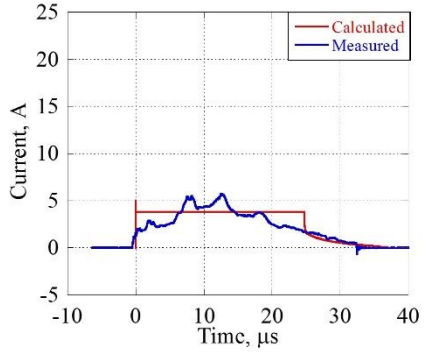

Fig. 23. Comparison of the flashover currents for V_0 = 1850V

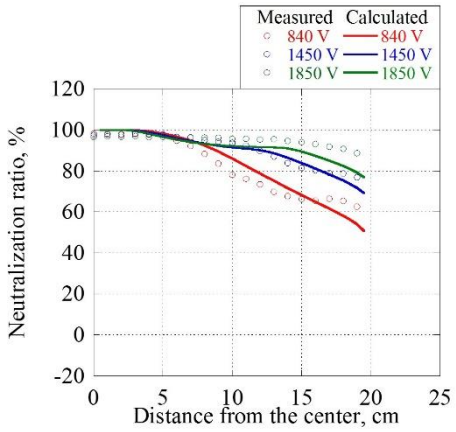

Fig. 24. Comparison of the neutralization ratio for each V_0

7. Conclusion

The ring coupon was uniformly charged by UV light (ozone type lamp). Then, electrostatic discharge triggered by laser was induced. The surface potential distribution before and after the discharge confirms that the discharge is propagating on the ring coupon concentrically from the discharge initiation point. The charge, stored on the surface of the ring coupon, was neutralized by the discharge plasma. From the test, the discharge current and the surface potential were measured. The neutralization range increased when the potential difference increased and the measured resistance showed the same characteristics as the simulation model results.

The simulation results of the flashover currents taking into account the plasma resistance did not match the experimental values. However, the simulated neutralization ratio of the surface potential showed similar characteristics with the experimental values.

For the differential voltages V_0 = 1450V and V_0 = 1850V, it was possible to approximate the charge, the current cut-off time, and the peak value to the experimental values by taking into account the inductance. However, for V_0 = 840V, it was not possible to approach the experimental values. It is considered to be due to the fact that in the current simulation model the inductance stays constant when the current increases. For future simulations, it would be better to consider the decrease of the inductance when the current increases. When the inductance is also taken into account with the plasma resistance, the neutralization ratio showed the same characteristics as the experimental values.

In the future, it is planned to calculate flashover current and neutralization ratio for larger coupon. The additional results will then be compared with the current model. Moreover, the number of experimental data used in the current simulation is not sufficient. Therefore, the discharge current and surface potential will be measured again, and the plasma resistance will be calculated. After the ring coupon discharge plasma model is determined, the discharge current and surface potential will be measured by using actual solar array coupon.

References

1) Hirokazu Masui, Kazuhiro Toyoda and Mengu Cho, “Electrostatic Discharge Plasma Propagation Velocity on Solar Panel in Simulated Geosynchronous Environment”.
2) T Okumura, M Imaizumi. *et al*.: Propagation Area and Speed of Flashover Discharge on Large Solar Array Panels in a Simulated Space Plasma Environment, 11th Spacecraft Charging Technology Conference, New Mexico, USA, September, 2010.
3) E. Amorin, D. Oayan, R. Sarrail, R. Reulet, “ Electrostatic Discharge On $1m^2$ Solar Array Coupon-Influence Of The Energy Stored On Coverglass On Flashover Current”, 9^{th} Spacecraft Charging Technology Conference, April, Tsukuba, 2005.
4) J. A. Young, M. W. Crofton: “ESD Propagation Dynamics on a Radially Symmetric Coupon”, 13^{th} Spacecraft Charging Technology Conference, June , California, 2014.
5) J. A. Young, M. W. Crofton,”Preliminary Measurement of ESD Propagation on a Round Robin Coupon”, 13^{th} Spacecraft Charging Technology Conference, June , California, 2014.
6) Tomonori Suzuki: “Research of Sustained Arc Test and Simulated Flashover Current” The 55th Symposium on Space Science and Technology Nov. 2011.
7) Kazuhiro Toyoda, Anna Kawano, Satoshi Miyazaki, and Mengu Cho: “Flashover discharge measurement with uniform surface charging and modeling of current waveform”, IEEE.